

Origin of ultra-compact dwarfs: a dynamical perspective

Hong-Xin Zhang^{1,2,3,4}, Eric W. Peng^{1,2}, Patrick Côté⁵, Chengze Liu^{6,7},
Laura Ferrarese⁵, Jean-Charles Cuillandre⁸, Nelson Caldwell⁹,
Stephen D. J. Gwyn⁵, Andrés Jordán¹⁰, Ariane Lançon¹¹, Biao Li^{1,2},
Roberto P. Muñoz^{10,11}, Thomas H. Puzia¹⁰, Kenji Bekki¹², John
Blakeslee⁵, Alessandro Boselli¹³, Michael J. Drinkwater¹⁴,
Pierre-Alain Duc¹⁵, Patrick Durrell¹⁶, Eric Emsellem^{17,18}, Peter
Firth¹⁴ and Ruben Sánchez-Janssen⁵

¹Department of Astronomy, Peking University, Beijing 100871, China
email: hongxin@pku.edu.cn

²Kavli Institute for Astronomy and Astrophysics, Peking University, Beijing 100871, China

³CAS-CONICYT Fellow

⁴Chinese Academy of Sciences South America Center for Astronomy, Camino El Observatorio
#1515, Las Condes, Santiago, Chile

⁵National Research Council of Canada, Herzberg Astronomy and Astrophysics Program, 5071
West Saanich Road, Victoria, BC V9E 2E7, Canada

⁶Center for Astronomy and Astrophysics, Department of Physics and Astronomy, Shanghai
Jiao Tong University, Shanghai 200240, China

⁷Shanghai Key Lab for Particle Physics and Cosmology, Shanghai Jiao Tong University,
Shanghai 200240, China

⁸Canada–France–Hawaii Telescope Corporation, Kamuela, HI 96743, USA

⁹Harvard-Smithsonian Center for Astrophysics, Cambridge, MA, 02138

¹⁰Instituto de Astrofísica, Facultad de Física, Pontificia Universidad Católica de Chile, Av.
Vicuña Mackenna 4860, 7820436 Macul, Santiago, Chile

¹¹Observatoire astronomique de Strasbourg, Université de Strasbourg, CNRS, UMR 7550, 11
rue de l'Université, F-67000 Strasbourg, France

¹²School of Physics, University of New South Wales, Sydney 2052, NSW, Australia

¹³Aix Marseille Université, CNRS, LAM (Laboratoire d'Astrophysique de Marseille) UMR
7326, F-13388 Marseille, France

¹⁴School of Mathematics and Physics, University of Queensland, Brisbane, QLD 4072,
Australia

¹⁵Laboratoire AIM Paris-Saclay, CNRS/INSU, Université Paris Diderot, CEA/IRFU/SAP,
F-91191 Gif-sur-Yvette Cedex, France

¹⁶Department of Physics & Astronomy, Youngstown State University, Youngstown, OH 44555

¹⁷Université de Lyon 1, CRAL, Observatoire de Lyon, 9 av. Charles André, F-69230
Saint-Genis Laval; CNRS, UMR 5574; ENS de Lyon, France

¹⁸European Southern Observatory, Karl-Schwarzschild-Str. 2, D-85748 Garching, Germany

Abstract. Discovery of ultra-compact dwarfs (UCDs) in the past 15 years blurs the once thought clear division between classic globular clusters (GCs) and early-type galaxies. The intermediate nature of UCDs, which are larger and more massive than typical GCs but more compact than typical dwarf galaxies, has triggered hot debate on whether UCDs should be considered galactic in origin or merely the most extreme GCs. Previous studies of various scaling relations, stellar populations and internal dynamics did not give an unambiguous answer to the primary origin of UCDs. In this contribution, we present the first ever detailed study of global dynamics of 97

UCDs ($r_h \gtrsim 10$ pc) associated with the central cD galaxy of the Virgo cluster, M87. We found that UCDs follow a different radial number density profile and different rotational properties from GCs. The orbital anisotropies of UCDs are tangentially-biased within ~ 40 kpc of M87 and become radially-biased with radius further out. In contrast, the blue GCs, which have similar median colors to our sample of UCDs, become more tangentially-biased at larger radii beyond ~ 40 kpc. Our analysis suggests that most UCDs in M87 are not consistent with being merely the most luminous and extended examples of otherwise normal GCs. The radially-biased orbital structure of UCDs at large radii is in general agreement with the scenario that most UCDs originated from the tidally threshed dwarf galaxies.

Keywords. galaxies: clusters, globular clusters, galaxies: nuclei, galaxies: elliptical and lenticular, cD, galaxies: kinematics and dynamics

1. Data and samples

This work is devoted to a comparative study of the dynamical properties of M87 UCDs, GCs and surrounding dwarf ellipticals. Our samples of 97 confirmed UCDs and 911 confirmed GCs within the central 1.5° of M87 are collected from both literature (e.g. Hanes *et al.* 2001; Strader *et al.* 2011) and our new observations. For new observations, we selected UCD and GC candidates for spectroscopic followup with Hectospec/MMT and 2dF/AAT based on the high-sensitivity ($g_{\text{lim}} = 25.9$ mag at 10σ for point sources) and high-resolution (FWHM $\sim 0.6''$ in i band) u^*griz imaging data from the Next Generation Virgo Cluster Survey (NGVS, Ferrarese *et al.* 2012).

The readers are referred to Zhang *et al.* (2015) for details of the samples and new observations. Briefly, our spectroscopic surveys of Virgo UCDs and GCs have been highly efficient, thanks to an unprecedentedly clean sample of Virgo UCD and GC candidates selected from NGVS. Our surveys covered nearly all of the area encompassed by one scale radius of the NFW dark matter halo toward the Virgo A subcluster ($2^\circ.143 = 0.617$ Mpc; McLaughlin 1999). Because the half-light radius $r_{h,\text{NGVS}}$ measurement for relatively faint sources is subject to large uncertainties, we only select UCDs with $g \leq 21.5$ mag and $r_{h,\text{NGVS}} \geq 11$ pc. In addition, sources with HST size measurement $r_{h,\text{HST}} > 9.5$ pc are also included as UCDs, irrespective of their brightness. All the other confirmed Virgo compact clusters are regarded to be GCs. Overall, our sample of UCDs is expected to be $\sim 60\%$ complete at $g_0 < 21.5$ mag. The median $(g - i)_0$ color of our samples of UCDs and blue GCs are 0.75 and 0.74 respectively, and about 92% of our UCDs fall into the color range of the blue GCs. So we place additional emphasis on a comparison between properties of UCDs and blue GCs in this work.

2. Results and discussion

Surface number density profiles. Our UCD sample is $\sim 98\%$ complete at $g_0 < 20.5$, which corresponds to $M_g < -10.6$. In Figure 1, we show the radial number density profiles of the 59 UCDs with $g_0 < 20.5$ mag, together with profiles of the photometrically selected blue GCs, red GCs ($g_0 < 24$ mag, Durrell *et al.* 2014) and the surrounding dE galaxies.

We adopted the Sérsic function to quantify (curves in Figure 1) the radial profiles of UCDs and GCs. Details about the profile fitting is described in Zhang *et al.* (2015). UCDs have a radial number density profile that is shallower than GCs in the inner $\sim 15'$ and as steep as the red GCs at large radii. The surrounding dE galaxies have much flatter and extended number density profiles than UCDs and GCs.

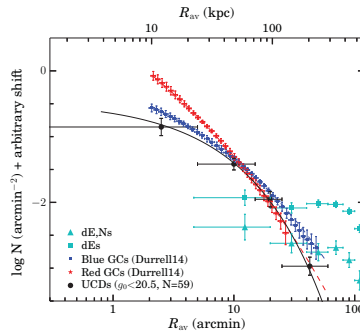


Figure 1. Radial number density profiles of UCDs (black), blue GCs (blue), red GCs (red), dE, Ns (cyan triangles) and all dE (cyan squares) galaxies. Overplotted on the data are the best-fit Sérsic profiles for UCDs and GCs. Note that radial profiles of the GCs have been vertically shifted down arbitrarily (2.1 for the blue and 1.7 for the red GCs) for comparison purpose.

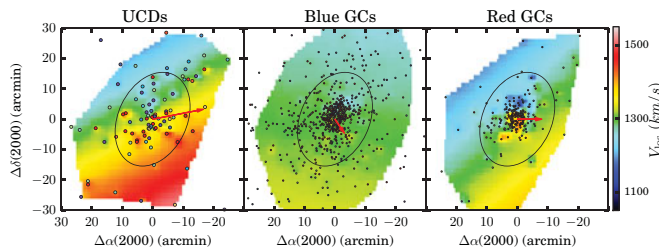


Figure 2. Spatial distribution of the UCDs (*left*), blue GCs (*middle*) and red GCs (*right*) are over plotted on their respective surface fitting (*the color background*) to the spatial distribution of line-of-sight velocities with the Kriging technique for the inner 30' of M87. The *black ellipses* represent the stellar isophotes of M87 at $10R_e$, and the *black solid line* marks the photometric minor axis of M87 in each panel. The *red arrows*, with the length being proportional to the rotation amplitude, mark the direction of rotation axis from our global kinematics fitting of v_{los} vs. PA to the inner 30'. The global kinematics fitting, which is primarily driven by the inner regions that contain most of the data points, matches the central velocity field from Kriging surface fitting. Among the three populations, the blue GCs seem to have an overall velocity field more aligned with the photometric major axis than the other two populations.

Velocity field. The UCDs and blue GCs have similar intrinsic velocity dispersion. The rotation amplitude of UCDs is more than 3 times stronger than that of the blue and red GCs. In addition, the overall velocity field of blue GCs is aligned with the photometric major axis of M87 much better than UCDs and the red GCs. Our test suggests that the probability of finding a rotation amplitude greater than or equal to the best-fit value for UCDs purely by chance is $\sim 2\%$, the probability for blue GCs is $\sim 27\%$, and $\sim 12\%$ for the red GCs. The significantly stronger rotation of UCDs as compared to GCs suggests that UCDs are kinematically distinct from GCs.

Orbital anisotropies. To constrain the orbital anisotropy profiles β_r of UCDs, blue and red GCs, we turn to the spherically symmetric Jeans equation. In determining β_r , we adopt the most recent determination of M87 mass profile by Zhu *et al.* (2014) based on made-to-measure modeling of over 900 M87 GCs. In addition, the surface number density profiles are de-projected to derive the 3D number density profiles which are used in solving the Jeans equation. Details of the Jeans modeling, including the functional form of β_r , can be found in Zhang *et al.* (2015). Basically, we used a maximum likelihood method to fit Jeans models to the observed $v_{\text{los},i}$ as a function of geometric average radius R_i , by assuming that $v_{\text{los},i}$ at R_i follows a Gaussian distribution. The most probable model β_r

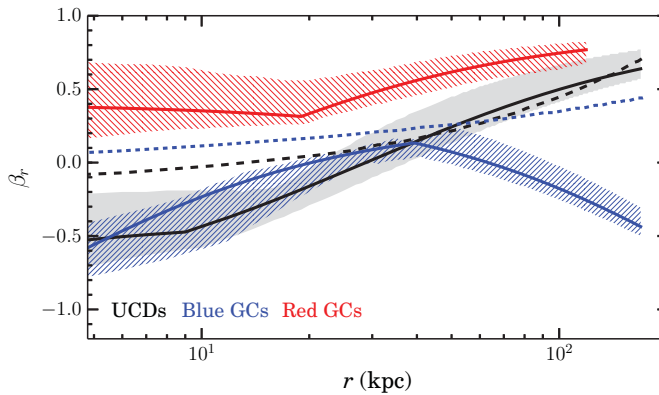


Figure 3. Variation of the anisotropy parameters as a function of the 3D radius. The profiles for UCDs, blue GCs, and red GCs are represented as black, blue, and red solid curves respectively. Following the same color code, the hatched regions of different styles mark the 68% confidence intervals for blue GCs, and red GCs. The grey shaded region marks the 68% confidence interval for the UCDs. The short dashed curves (*black* for UCDs, *blue* for blue GCs) represent the anisotropy profiles predicted by a universal relation between the number density slope and β for relic high- σ density peaks as found in cosmological simulations by Diemand *et al.* (2005).

profile for each population is taken as the fiducial one, and the 68% confidence intervals are determined by randomly resampling the real data sets, with $\sim 10\%$ of data points being left out for each resample.

The determined β_r profiles for UCDs, blue and red GCs are shown in Figure 3. The UCD system has an anisotropy profile that becomes more radial with radius, with β_r being negative within the inner ~ 40 kpc and being positive beyond. The blue GCs have a radially increasing β_r profile in the inner ~ 40 kpc but a radially decreasing profile at larger radii. Among the three populations, the red GCs exhibit the largest radially-biased orbital structure across the explored radius range.

Although being more negative in the innermost radii, the β_r profile of UCDs determined from Jeans analysis is more or less consistent with the cosmological simulations of Diemand *et al.* (2005). In contrast, the blue GCs exhibit large deviation from the cosmological simulations. The significantly tangentially-biased orbital structure of UCDs at small radii can be partly attributed to a strong tidal transformation. The finding that the blue GCs are tangentially-biased, rather than radially-biased, at large radii may indicate that the blue GCs in the outer halo of M87 have not yet established an equilibrium state and is still in an early and active stage of assembly by continuously accreting the surrounding dwarf galaxies (e.g. Côté, Marzke & West 1998).

3. Conclusion

We conclude that most UCDs in M87 are not consistent with being merely the most luminous and extended examples of otherwise normal GCs. The radially-biased orbital structure of UCDs at large radii is in general agreement with the scenario that UCDs are tidally stripped nuclei of dwarf galaxies. The distinct rotational properties of UCDs, as compared to GCs and the surrounding dE galaxies, indicate that the primary UCD progenitors do not necessarily resemble the present-day surviving dwarf galaxies.

References

- Côté, P., Marzke, R. O., & West, M. J. 1998, *ApJ*, 501, 554
 Diemand, J., Madau, P., & Moore, B. 2005, *MNRAS*, 364, 367

- Durrell, P. R., Côté, P., Peng, E. W., *et al.* 2014, *ApJ*, 794, 103
Ferrarese, L., Côté, P., Cuillandre, J. -C., *et al.* 2012, *ApJS*, 200, 4
Hanes, D. A., Côté, P., Bridges, T. J., *et al.* 2001, *ApJ*, 559, 812
Strader, J., Romanowsky, A. J., Brodie, J. P., *et al.* 2011, *ApJS*, 197, 33
Zhang, H. -X., Peng, E. W., Côté, P., *et al.* 2015, *ApJ*, in press, arXiv: 1501.03167
Zhu, L., Long, R. J., Mao, S., *et al.* 2014, *ApJ*, 792, 59